Energy Equip. Sys. / Vol. 10/No. 1/March. 2022/ 27-40

ENERGY EQUIPSYS

Energy Equipment and Systems

http://energyequipsys.ut.ac.ir
www.energyequipsys.com

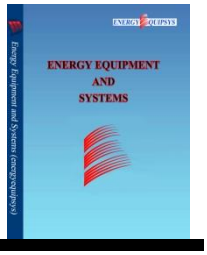

Investigation of thermal performance and entropy generation in a microchannel heatsink with a wavy channel using bio nanofluid

Authors

Akram Jahanbakhshi [a]
Afshin Ahmadi Nadooshan [a*]
Morteza Bayareh [a]

[a] Department of Mechanical Engineering, Shahrekord University, Shahrekord, Iran

Article history:

Received : 12 May 2021
Accepted : 9 July 2021

ABSTRACT

In the present study, two cases of a microchannel heat sink are studied: i) with 50 wavy channels, and ii) with the addition of wavy tubes. Also, the effect of nanofluid Ag/water-ethylene glycol 50% is investigated. ANSYS Fluent software was used to solve the equations expressed in the problem geometry. To solve the momentum equation, the second-order UPWIND method is used. Also, the SIMPLEC algorithm with a staggered pressure grid is employed to couple velocity and pressure fields. The results show that the addition of a microtube significantly increases the overall thermal coefficient of the system because despite the microtube and having two different geometries in a heatsink at the same time, the heat exchange between the body and the fluid increases so that in a flow without a microtube with Reynolds number 300, the average surface temperature is 315 K, but the addition of a microtube reduces this temperature to 309 K^0, which is equal to 6 degrees. Also, as the Reynolds number (Re) increases, the effect of increasing the concentration of nanoparticles enhances. The results demonstrate that the thermal entropy generation (S_h) decreases at high values of Re. In addition, the decrease in frictional entropy generation (S_f) due to the increase in nanoparticles is directly related to their concentration and independent of Re. So that the Percentage of decrease in friction entropy due to an increase in nanoparticle concentration relative to the pure fluid is equal to 1% for a concentration of 0.1% and 9% for a concentration of 1%. It is revealed that total entropy generation (S_{tot}) and S_f do not exhibit the same behavior.

Keywords: Numerical Study, Micro Heatsink, Entropy, Wavy Channel, Bio Nanofluid.

1. Introduction

With the development of science and technology, researchers have found that some advantages are obtained by reducing the size of devices: compact size, easy access and transportation, and enhancement of system performance. For this reason, many researchers analyzed micro-scale flow and have made great efforts to reduce the size of the equipment and their optimization.In addition to their high capability, these compact devices also have high energy consumption and require more power and smaller cooling systems. The micro-channel heatsink, which is known as one of the cooling methods with a high heat transfer coefficient (h), provides good conditions for removing heat flux due to the small geometric dimensions and the high surface-to-volume ratio of the channel [1-3]. A heatsink is a heat exchanger that

* Corresponding author: Afshin Ahmadi Nadooshan
Department of Mechanical Engineering, Shahrekord University, Shahrekord, Iran
Email: ahmadi@sku.ac.ir

transfers thermal energy from a high-temperature device to a lower-temperature fluid environment. Heatsinks are widely used to dissipate heat and improve energy efficiency in electrical equipment because the power source of electronic equipment has not the efficiency of 100% and produce additional heat, which is often detrimental to the operation of the device. Therefore, extensive experimental and analytical studies have aimed at developing design methods to change the geometry of the heatsink to achieve maximum efficiency. In addition, using the analysis of the second law of thermodynamics and calculating the entropy generation is useful in design and optimization. In recent research, wavy microchannels have also attracted a great deal of attention because they have a significant heat transfer rate compared to straight channels. The secondary flow formed by the curved surfaces causes a mixture between the fluid near the wall and the fluid in the center of the flow, which is the reason for the improvement of the thermal performance of these surfaces [1].

In 1981, Tuckerman and Pease [2] concluded that reducing the size of the cooling channel to the micron scale increases heat transfer. They proposed a microchannel to increase thermal performance. They stated that there is an inverse relationship between h and channel length characteristic; heat transfer increases with decreasing microchannel hydraulic diameter. Toh et al. [3] studied the steady-state flow and heat transfer equations using the finite volume method. Their results showed that the input heat transfer reduces friction losses and viscosity at low values of Re, leading to an increase in the water temperature. Peng and Peterson [4-5] conducted an experimental study of pressure drop and convective heat transfer in a rectangular microchannel. They concluded that in laminar and turbulent flows, the aspect ratio of the cross-sectional area has a significant effect on the friction of the flow and heat transfer. In 2015, Duryodhan et al. [6] performed a three-dimensional numerical and experimental study of a single-phase fluid in convergent and divergent microchannels for cooling electronic components. In this study, they evaluated the Nusselt number (Nu) and measured the surface temperature and the liquid mass to obtain h. Their study showed that under the same conditions, the heat transfer in the convergent channel is 35% higher than that in the divergent one. Also, the pumping work for convergent and divergent channels is less than that for simple channels.

Pourmehran et al. [7] evaluated the thermal performance of two-dimensional porous rectangular microchannel heatsink using copper- and alumina-water nanofluid numerically and revealed that as the volume fraction (ϕ) of nanoparticles and the inertial force increase, Nu increases. In an analytical-numerical study, Hatami and Ganji [8] examined the cooling, the thermal conductivity of a porous rectangular microchannel using copper-water nanofluid and showed that wider fins decrease nanofluid temperature and fin temperature, resulting in an increase of Nu. Lam and Prakash [9] numerically examined heat transfer and entropy generation of the forced convection heat transfer of fluid on the inner surface of a channel in a porous medium. The coolant was a laminar output flow of a jet. Their results showed that the highest entropy generation is due to the irreversibility of fluid friction, and the average Nu increases with increasing the Darcy number and the thickness of the porous layer, as well as with decreasing channel height and porosity coefficient. Ting et al. [10] studied the production of entropy of aluminum oxide water flow in a rectangular microchannel, filled with porous medium and taking into account the effects of solid-phase heat production. They demonstrated that with the increase in the amount of heat production, the irreversible solid phase increases significantly. Kalteh and Abedinzadeh [11] showed that by increasing Re from 5 to 25 and by increasing ϕ from zero to 4%, the heat transfer performance is improved by 19 and 17%, respectively. They found that increasing the Hartmann number also increases the average Nu. Guo [12] used the second law of thermodynamics and found that the parameters of the curved channel have a significant effect on its thermodynamic performance. Hung et al. [13] also found that the rate of heat transfer improved significantly with increasing the frequency or decreasing the curvature wavelength.

Hung et al. [14] revealed that the maximum heat transfer performance of a heatsink

corresponds to alumina, which is approximately 22% higher than the base fluid. They concluded that the use of water as a based fluid with less dynamic viscosity than ethylene glycol improves thermal performance. They also stated that the lowest thermal resistance is achieved at a volume concentration of 2% and the pump power consumption of 0.5 W. Naphon et al. [15] demonstrated that the average heat transfer rate of nanofluid is higher than the base fluid and the pressure drop increases slightly with ϕ. Chein and Chen [16] examined the effect of inlet and output flows in a microchannel heatsink with rectangular microchannels. They first examined a conventional arrangement with straight input and output. Then they chose five other arrangements. The dimensions of the geometry are the same for all six arrangements, but the location of the flow in and out of them varies. They showed that the inequality of the velocity distribution in the microchannels for arrangements in which the fluid enters the heatsink horizontally is greater than that for the arrangements in which the fluid enters the thermal sink vertically. They also showed that the V-shaped arrangement performs the best due to its thermal resistance.

In recent years, microchannel heatsink (MCHS) developed by Tokerman and Passe have become one of the most widely used cooling methods in microelectronic equipment. Numerous studies have been conducted in this regard, such as the theoretical study of Knight et al. [17] who have optimized MCHS. Elvakumar and Suresh [18] examined the effects of water-copper oxide nanofluid on a heatsink with thin channels under constant heat flux. They found that h increases with increasing ϕ in the water-based fluid, and the pump power consumption increases by 15.11% for the nanofluid with a volumetric concentration of 2%. Mostafa et al. [19] examined the effect of slip boundary conditions on entropy generation for Newtonian and non-Newtonian fluid flows in a channel with parallel plates. In a numerical study, Khorasanizadeh and Sepehrnia [20] examined the effect of four different input/output flow arrangements on cooling an electron chip using a three-dimensional porous microscopic trapezoidal microchannel heatsink. They showed that using a porous medium is effective in reducing chip temperature. In another study, Khorasanizadeh et al. [21] studied a heatsink consisting of seven microchannels with an equilateral triangular cross section. They examined two horizontal and vertical entry and exit arrangements and found that the thermal performance, in addition to the input and output arrangement, depends on the shape and geometry of the microchannels. Ghasemi et al. [22] investigated the combined heat transfer during the three-dimensional and laminar flow of alumina nanofluid in mixed convection in a triangular microchannel. Their results showed that increasing ϕ increases heat transfer and friction coefficients while decreases the thermal resistance. Lin et al. [23] used a numerical method to design a heatsink with wavy channels. They proposed the most suitable geometry for a constant pumping power of the system by changing the wavelength and frequency of the channels. These studies have shown that MCHS performs much better than conventional energy absorbers, but they still need to be studied and improved. Nemati et al. [24] investigated the performance coefficient of the system as the key parameter of the first law of thermodynamics and the exergy efficiency as the key parameter of the second law of thermodynamics. In 2017, Zuo and Yu [25] proposed a method to optimize the performance of thermoelectric modules as a function of entropy generation rate. In this study, the effects of air pressure drop inside the heat exchanger were considered and the optimal performance for different electric currents applied to the module as well as different thermal capacities for heat exchangers were investigated. Delsman et al. [26] optimized the heatsink geometry of the plate to achieve the best performance in terms of flow distribution. In a numerical study, Haddad et al. [27] studied the entropy generation due to the forced continuous linear convection in the passage of fluid through the microchannel. Chuan [28] examined the characteristics of fluid flow and heat transfer for a microchannel heatsink in the presence of porous fins. Shaeri and Yaghoubi [29] modeled a three-dimensional heatsink for turbulent flow regime. They examined vortices and temperature fields. This modeling was also performed for normal and porous fins at different values of Re and the results were compared. Micheli et al. [30] examined heat

transfer in a heatsink with a needle fin and heatsink with flat plates, and compared the two models. They found that the effective coefficient of using fins is between 3% and 7%. Also, heat is better transferred from heatsinks with needle fins. In a numerical study, Ebrahimi et al. [31] studied heat transfer from vortex generators by water- aluminum oxide and water-copper oxide nanofluids compared to pure water. Their results showed an increase in heat transfer from 2.29% to 30.63% for water-aluminum oxide and an increase from 9.44% to 53.06% for copper oxide compared to pure water.

Various properties of new nanofluids obtained from the combination of nanoparticles added to the base fluid, such as thermal conductivity, viscosity, and electrical conductivity, have been reported in various experimental investigations based on the concentration of nanoparticles, temperature, and the properties of the base fluid. [32]. Al-Rashed et al. [33] studied the effect of nanofluid at different values of Re and obtained different values for the wavy channel by examining different geometric parameters for the microchannel.

In the present work, the optimal geometry introduced by Al-Rashed et al. [33] is used as the reference geometry and the effect of adding of microtube along with microchannel and the use of Ag/water-ethylene glycol 50% nanofluid is studied. The nanofluid used can be prepared by biological synthesis and is known as a bio method. In fact, one of the innovations of this study is the use of microtubes along with microchannels and the study of two different geometries in a heatsink and investigation of thermal performance and entropy generation in this heatsink.

Nomenclatures

L_X	The length of the micro heatsink in the x direction(mm)
L_Y	The length of the micro heatsink in the Y direction (µm)
L_Z	The length of the micro heatsink in the z direction (mm)
W_C	Microchannel width (µm)
H_f	The distance of the microtube from the floor (µm)
H_D	Distance of the center of the micro tube from the floor (µm)
H_C	The length of the microchannel section (µm)
D	The diameter of the microtube (µm)
a_W	Wave amplitude (µm)
l_W	Wavelength (mm)
$\vec{u}$	Velocity vector (m/s)
θ	Dimensionless parameter CPU surface temperature uniformity
ρ	Density (kg/m³)
C_p	Specific heat capacity (J/kg K)
μ	Viscosity (Kg/m.s)
k	Thermal conductivity (W/m.K)
ϕ	The volume fraction of nanoparticles
$T_{CPU,Max}$	Maximum CPU surface temperature (K^0)
$T_{CPU,Mean}$	Average CPU surface temperature (K^0)
$T_{CPU,min}$	Minimum CPU surface temperature (K^0)
T_{in}	Inlet temperature (K^0)
h	Overall heat transfer coefficient of thermal wells (W/m^2K)
W_{pump}	Total pumping power (W)
S_{gen}	Total entropy generation (mW/K)
S_h	Thermal entropy (mW/K)
S_f	Frictional entropy (mW/K)
S_q	Wall heat flux entropy (mW/K)
q''	Heat flux (W/m^2)

2. Nanofluid properties

Sarfaraz and Hormozi [34] prepared silver nanoparticles using tea leaves, which is a pure method. In the present study, according to their work, a mixture of 50% water and ethylene glycol is used as the base fluid and silver nanoparticles are employed as nanoparticles. Also, the calculations of the properties of the nanofluid mixture are performed based on their investigation.

Density, specific heat capacity, viscosity, and thermal conductivity are calculated using the following equations:

$$\rho_{nf} = (1-\phi)\rho_{bf} + \phi\rho_p \quad (1)$$

$$\rho_{nf}C_{p,nf} = (1-\phi)\rho_{bf}C_{p,bf} + \phi\rho_p C_{p,p} \quad (2)$$

$$\mu_{nf} = \mu_{bf}(1 + 2.5\phi) \quad (3)$$

$$k_{nf} = k_{bf}[0.981 + 0.00114T(°C) + 30.661\phi] \quad (4)$$

where ρ is the density, C_p the specific heat capacity, μ the viscosity, k the thermal conductivity, T is the temperature. Subscripts *bf*, *p*, and *nf* refer to base fluid, nanoparticles, and nanofluid, respectively.

3. Description of the model

3.1. Geometry and boundary conditions

A schematic of the heatsink considered in the present study is shown in Fig. 1. Two cases of microchannel heatsink are studied: i) with 50 wavy channels, and ii) with the addition of wavy tubes.

Due to the symmetry of the problem, only a part containing one channel and two half-tubes of the problem is solved, In such a way that the walls of the channel have surface symmetry and the middle plane of the two half-tubes are coupled to each other. Due to that the plane symmetry is on the solid fin, the value of the temperature gradient perpendicular to the plane is zero in the equations. To coupling the middle plane of two half-tubes in the iteration process, the difference in velocity, temperature, and pressure components on these two planes are equal to zero. Table 1 presents the value of the dimensions specified in Fig. 1.

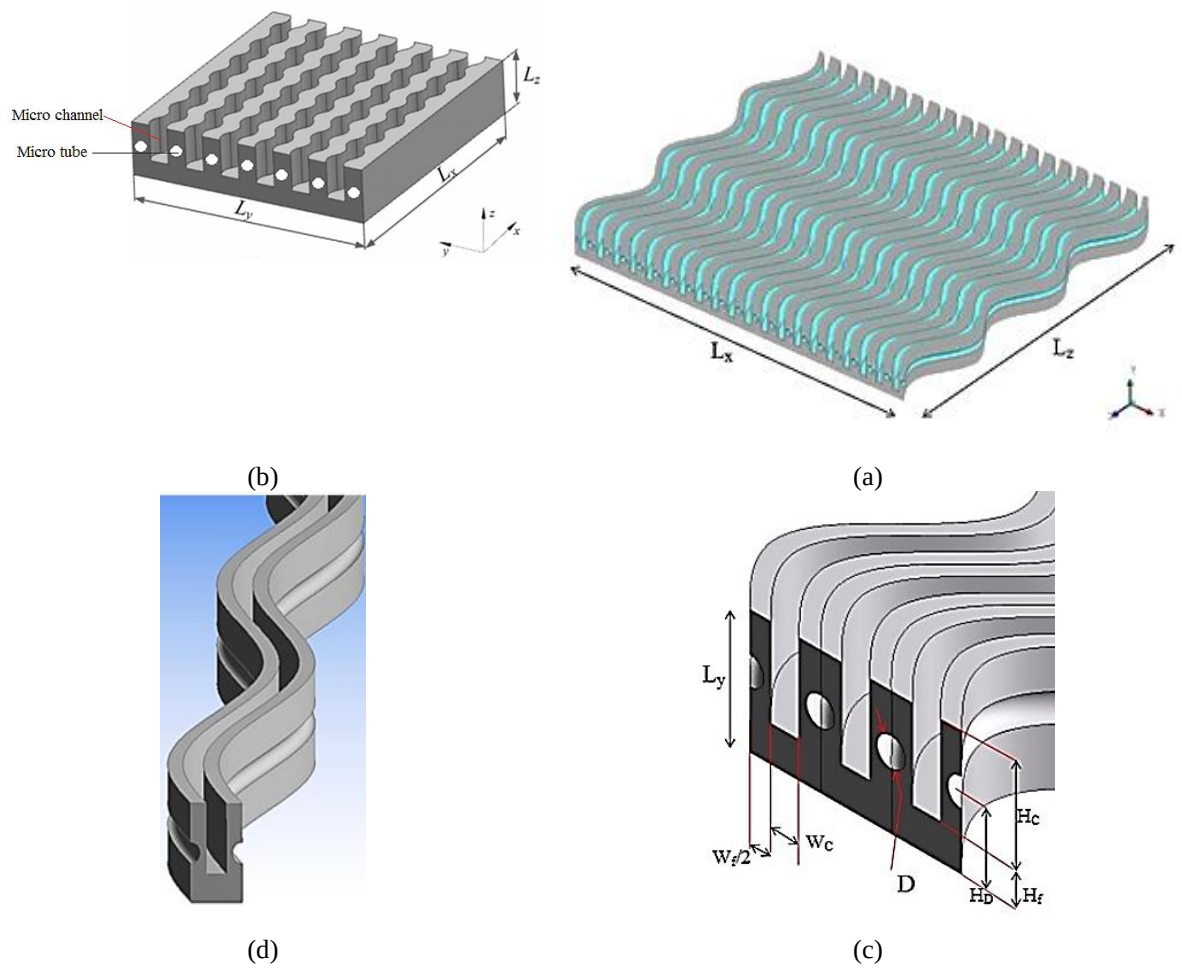

Fig. 1. (a)Schematic of the problem in the present work,(b) Viewing micro-tubes and micro-channel, (c) Geometrical parameters, and (d) Computational area according to the symmetry of the general geometry

Table 1. Dimensional parameters of the problem.

Parameter	Value
LX	10mm
LY	350μm
LZ	15mm
Wf	120 μm
WC	80 μm
D	80 μm
Hf	100 μm
HC	250 μm
HD	200 μm

It is assumed that this heatsink is located on a CPU, and therefore only its bottom surface is subjected to heat flux of 50 W/cm^2. The flow inlet temperature is also assumed to be 300 K^0. all surfaces of heat wells, including sidewalls and upper walls that are in contact with the surrounding environment, are considered insulation.

For the inlet boundary condition in a given Reynolds (300, 500, 700, 1000, and 1500), the uniform inlet velocity (u) is calculated, the other two velocity variables (v, w) are set to zero, And the inlet pressure gradient is defined as zero.

In the present study, the current is incompressible and as a result, in the absence of return current, there is no output condition and it is obtained as an extrapolation from the momentum and continuity equation.

$$Re = \frac{\rho u D}{\mu} \tag{5}$$

Here D is a "characteristic width" of the channel, defined as

D=4. (cross-sectional area)÷(perimeter p).

The waveform of the channel and tube along the heatsink is a sinusoidal function (Eq. 6) [33]:

$$S(z) = a_W \sin\frac{2\pi z}{L_W} \tag{6}$$

In this study, according to the reference [33], the values of $a_W = 138\mu m$ and $L_W = 5mm$ are considered for channel and tube along with the heatsink. Also, the Re of the microchannel is 10 times that of the microtube.

3.2. Governing equations

The present study evaluates the entropy generation and thermal behavior of Ag/water-ethylene glycol 50% nanofluid with ϕ = 0.1%, 0.5%, and 1%. For this purpose, it is necessary to solve the governing equations of mass, momentum, and energy

To solve the equations for fluid flow and heat transfer, the following assumptions are considered**:**

1. Fluid flow and heat transfer are three-dimensional and steady state
2. Nanofluid flow is laminar and single phase
3. Nanofluid is considered as a Newtonian and incompressible fluid

According to the mentioned assumptions of the continuity equation, the momentum equations in the three directions x, y, and z as well as the energy equations in the fluid part and the solid part of the heat well are expressed as follows [33]:

Continuity equation:

$$\nabla.\left(\rho_{nf}\vec{u}\right) = 0 \tag{7}$$

Momentum equation:

$$\nabla.\left(\rho_{nf}\vec{u}\vec{u}\right) = -\nabla p + \nabla.\left(\mu_{nf}\nabla\vec{u}\right) \tag{8}$$

Energy equation for fluid phase:

$$\nabla.\left(\rho_{nf}\vec{u}C_{p,nf}T\right) = \nabla.\left(k_{nf}\nabla T\right) \tag{9}$$

Energy equation for solid phase:

$$\nabla.\left(k_s\nabla T\right) = 0 \tag{10}$$

where, $\vec{u}$ is the velocity vector and p is the pressure. The subscript s refers to the properties of the solid phase.

In order to calculate entropy, integral and differential forms are considered according to the Siakiaquoli et al. [35] and Began [36]. The amount of entropy generation in this study is calculated using both methods. Thus, the computational process is ensured. It is also seen that to calculate S_{tot}, the integral method is more accurate and its calculations will be less sensitive to the type of grid. The amount of entropy generation in the integral form is obtained by calculating the following equations on the system boundaries [35-36]:

$$S_{gen} = S_h + S_f - S_q \tag{11}$$

$$S_h = \dot{m}\int_{in}^{out} c_p\frac{dT}{T}$$

$$S_f = \dot{m}\int_{out}^{in}\frac{v}{T}dP$$

$$S_q = \oint_A \frac{dQ}{T}$$

Since the studied geometry has several inputs and outputs, the equations are considered as follows:

$$S_h = \sum_{outlets} \iint_{S_{outlet}} \rho V C_p Ln\, T\, dA - \sum_{inlets} \iint_{S_{inlet}} \rho V C_p Ln\, T\, dA \quad (12)$$

$$S_f = \sum_{inlets} \iint_{S_{inlet}} \frac{VP}{T}\, dA - \sum_{outlets} \iint_{S_{outlet}} \frac{VP}{T}\, dA \quad (13)$$

$$S_q = \oint_A \frac{q''}{T} dA \quad (14)$$

By defining the parameter θ as Eq. 15, the uniformity of the CPU surface temperature cooled by the heatsink can be controlled by defining the parameter θ (Eq. 15). As the value of θ decreases, the surface temperature of the heatsink is more uniform.

$$\theta = \frac{T_{CPU,Max} - T_{CPU,min}}{T_{CPU,Mean}} \quad (15)$$

where $T_{CPU,Max}$, $T_{CPU,Mean}$ and $T_{CPU,min}$ are maximum, mean, and minimum CPU surface temperature, respectively. Convective heat transfer coefficient is defined as follows [33]:

$$h \equiv \frac{q''}{T_{CPU,Mean} - T_{in}} \quad (16)$$

4. Numerical method

ANSYS Fluent 18.0 software is employed to solve the governing equations. The second-order upwind method is used to solve the momentum equation and the SIMPLEC algorithm with the staggered grid is employed for coupling pressure and velocity fields. The convergence criterion is set at 10^{-8} for the energy equation and 10^{-6} for the other equations based on the scaled residuals.

The independence of the grid is investigated. Table 2 shows the results for channel and tube Reynolds numbers of 700 and 70, respectively, when ϕ = 1%.

Based on Table 2, the grid resolution of 195,000 is selected for further simulations (Fig.2).

The present work is verified with the experimental results of Sui et al. [37].

Table 2. Grid study results.

Number of elements	ΔT [K]	W_{pump} [W]
24000	3.386	0.0186
27000	3.387	0.0475
74000	3.388	0.0568
128000	3.388	0.0587
195000	3.388	0.0591
330000	3.388	0.0591

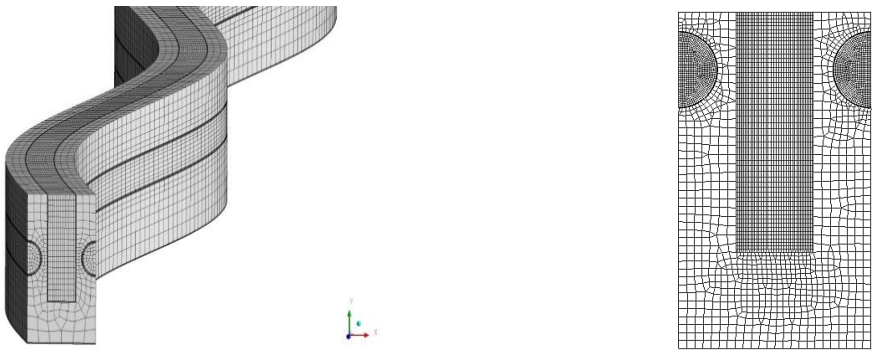

Fig. 2. An image of the calculation region and grid used for the current simulations.

Figure 3 illustrates a comparison between Nu calculated by present numerical simulations and the one reported by Sui et al. [37]. According to this paper, a wavy microchannel is modeled based on the parameters presented in Table 3. A comparison between the amount of Nu calculated by numerical solution and the experimental results of Sui et al. [37] is shown in Fig. 3. This figure reveals that the present results are in good agreement with experimental data. The maximum error between the present study and the experimental data is 8%, which is related to the flow with Re = 300. For Re = 500, the error is 3% and for Re = 700, the present results are matched with the experimental data.

Table 3. Geometric parameters of the validation problem.

Parameter	Value
W_f	193 µm
W_C	207 µm
H_f	100 µm
H_C	406 µm
a_W	138 µm
L_Z	25 mm

5.Results and discussions

The current numerical study aims to investigate the hydraulic and thermal behavior of a wavy microchannel heatsink with Ag/water-ethylene glycol (50%) nanofluid for cooling digital processors. The effect of microtubules on the heatsink performance is also investigated. The simulations are based on different values of ϕ (0%, 0.1%, 0.5% and 1%) and various values of Re (300, 500, 700, 1000 and 1500).

The variation of h is presented in Fig. 4 for the heatsink with and without microtubes at different values of Re and various values of ϕ. The dashed lines correspond to the ones without microtubes and solid lines are for that with the microtubes. The figure shows that h increases by increasing ϕ for all cases. On the other hand, as Re increases, the effect of ϕ becomes stronger.

It is found that the addition of microtubes results in a significant increase in the overall thermal coefficient of the system such that h for the system with microtubes at Re = 500 and 700 is 80% and 110% higher than that without microtubes at Re = 1000 and Re = 700, respectively. This is due to that the presence of microtubes along the channel increases the heat exchange between the heatsink body and the fluid. On the other hand, the separation of the microchannel and tube paths and the creation of higher temperature mixing in the fluid stream cause the fluid temperature to increase along the channel wall decreases. In other words, the temperature difference between the fluid and solid does not decrease significantly, leading to an increase in the rate of heat transfer.

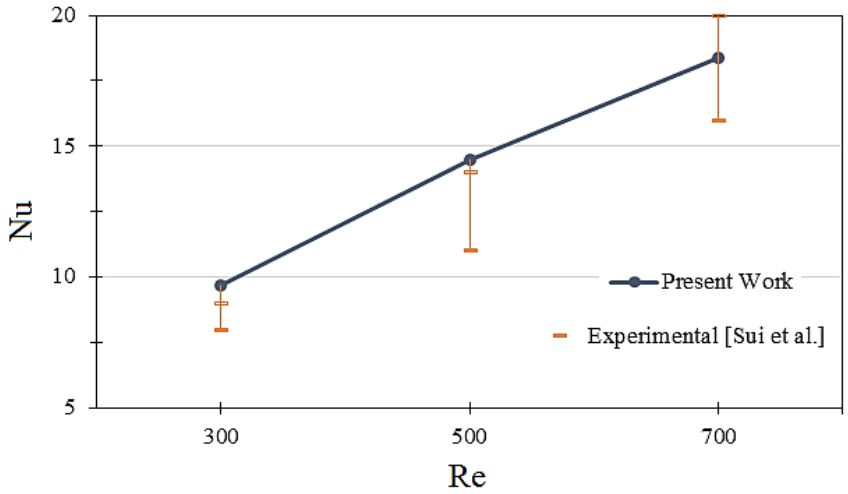

Fig. 3. Nu versus Re.

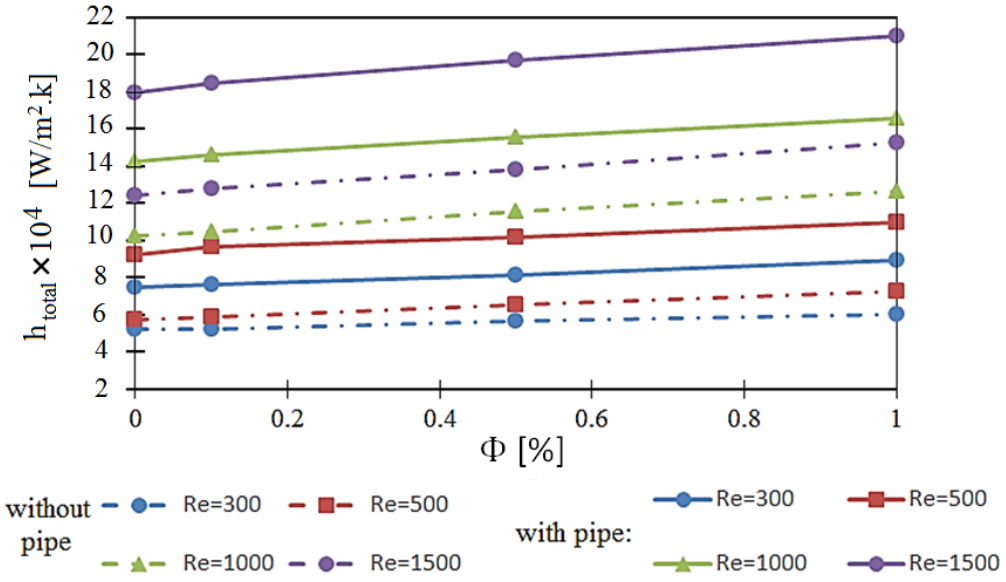

Fig. 4. The variation of h_{total} for the heatsink with and without microtubes at different values of Re and various values of ϕ.

The enhancement effect of nanoparticles and microtubes can also be investigated based on the average and maximum temperature of the CPU surface. As ϕ increases, the heat transfer performance of the CPU is improved, leading to a reduction in the surface temperature. This is due to that a low-temperature gradient is required to transfer the heat generated by the processor (Fig. 5). Figure 5 shows the decreasing trend of the average surface temperature due to the addition of nanoparticles. The performance of nanoparticles at lower Re is better: the addition of nanoparticles at lower values of Re causes the processor surface temperature to change more. On the other hand, the addition of microtubules leads to a much stronger performance. For example, in a heatsink without microtubes, the mean temperature of the CPU surface is 315 K at Re = 300. The addition of microtubes causes the temperature to decrease by 309 K, while the addition of 1% nanoparticles reduces the surface temperature by 313 K.

Figure 6 illustrates the ratio of temperature distribution to an average temperature of the CPU surface. A smaller ratio leads to more uniformity of the temperature distribution on the CPU surface. Due to the increase in h due to the addition of nanofluid to the system, the thermal performance is improved. It is also observed that the temperature is more uniform on the surface, but there is an inverse relationship between the effect of nanofluid concentration and flow rate. As Re increases, the flow uniformity enhances due to the stronger effect of convection in the flow. Therefore, the effect of the nanofluid addition will not be significant. On the other hand, the use of a microtube tube has led to a more uniform distribution of the temperature of the CPU surface due to the increase in heat transfer rate and the reduction of the thermal resistance of farther areas of the processor. For example, the surface temperature distribution for a flow with a microtube at Re = 700 is more uniform than a flow without a microtube at Re = 1500.

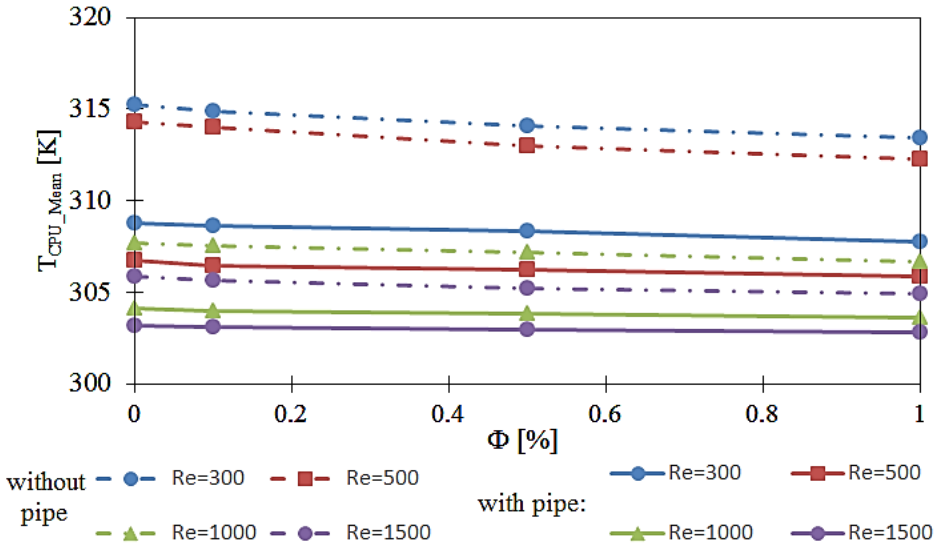

Fig. 5. Mean temperature of CPU surface for different values of ϕ.

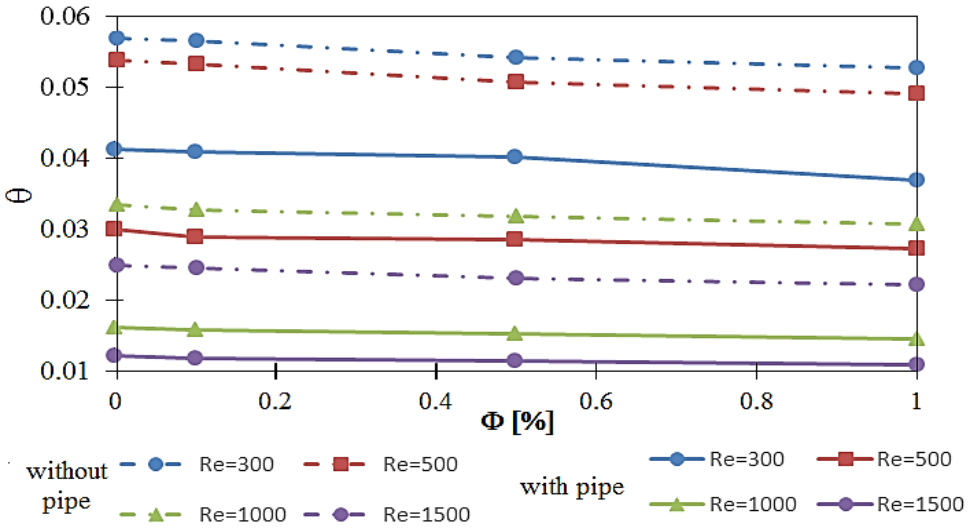

Fig. 6. Flow uniformity according to parameter θ.

The amount of entropy generation in the heatsink with the tube is calculated based on the integral method. At this step, the main purpose is to study the trend of changes and compare Figs. 7 to 10. Figure 7 shows that, regardless of the concentration of nanoparticles in the fluid, an increase in Re leads to an increase in the entropy generation, which is due to S_f. The variation of S_f is shown separately in Fig. 8. As shown in this figure, the amount of S_f has a relationship of the second-order by Re ($S_f \propto Re^2$). Also, the decrease in S_f due to the increase in ϕ has a direct relationship with its concentration, because with increasing volume fraction, the average velocity of nanofluid generally decreases and the friction entropy changes decrease and independent of Re. This percentage decrease is shown in Table 3.

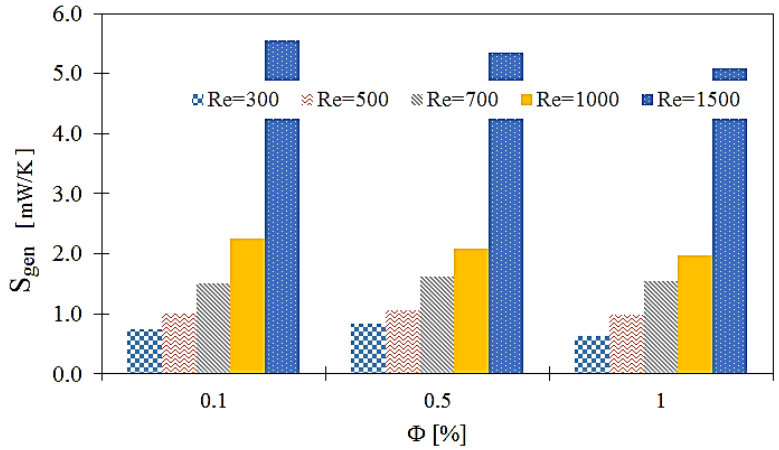

Fig. 7. Amount of entropy generation in the heatsink.

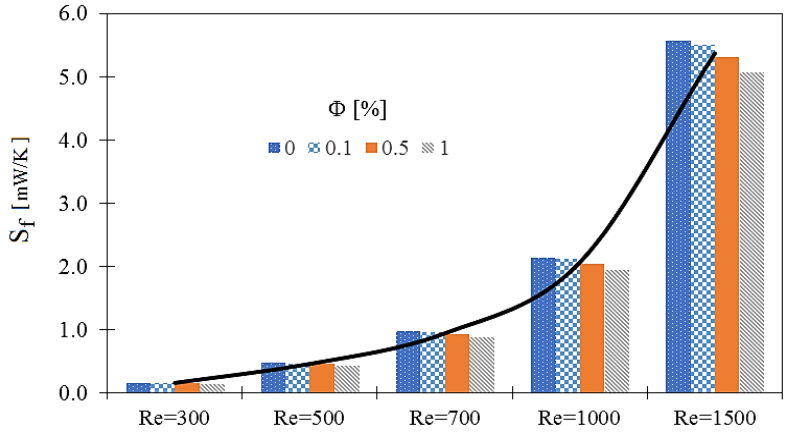

Fig. 8. S_f for different values of Re and various values of ϕ.

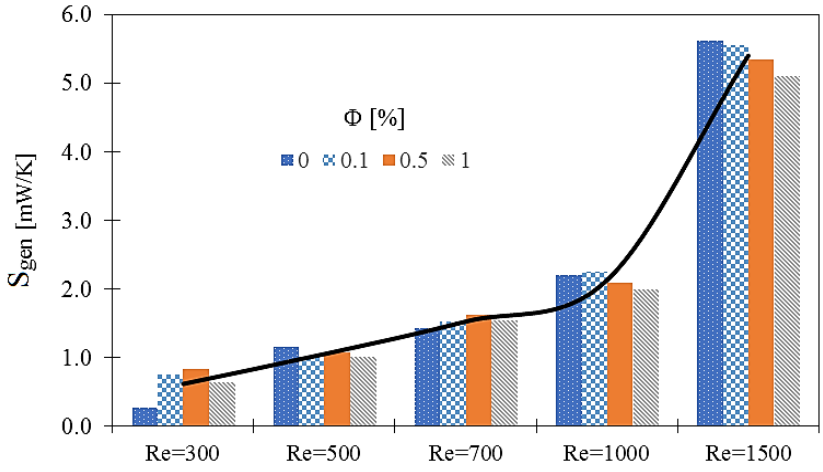

Fig. 9. Entropy generation versus Re.

Table 3. The percentage decrease in Ef due to ϕ.

ϕ (%)	0.1	0.5	1
Percentage decrease compared to pure fluid (%)	9	4.7	9

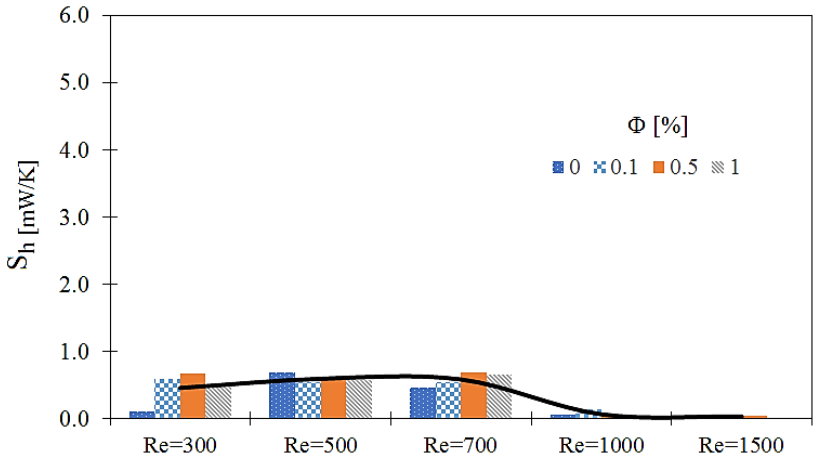

Fig. 10. S_h for different values of Re.

By evaluating the entropy generation in terms of Re, it is found that S_{tot} and S_f do not have the same behavior (Fig. 9). The values of S_{tot} show a relationship of the third order with Re ($S_{gen} \propto Re^3$) and regular behavior is not observed due to the addition of nanofluid. Fig. 10 shows the amount of E_{th}. The figure demonstrates a decrease in the rate of E_{th} in the flow as the flow rate increases and the temperature difference between the wall and the fluid decreases.

6. Conclusion

In the present study, two cases of a microchannel heatsink were studied: i) with 50 wavy channels, and ii) with the addition of wavy microtubes. Also, the effect of nanofluid Ag/water-ethylene glycol 50% was investigated. Comparing the two cases of the heatsink with and without microtube demonstrated that the addition of the microtube causes a significant increase in the overall thermal coefficient of the system. It was also concluded that by increasing the concentration of nanoparticles and improving heat transfer performance, the surface temperature of the processor decreases. This was due to that there is a small temperature gradient to transfer the heat from the processor to the fluid. It was revealed that regardless of the concentration of nanoparticles in the fluid, an increase in Re results in an increase in the entropy generation, which seems to be due to S_f. By evaluating the entropy generation in terms of Re, it was observed that S_{tot} and S_f do not exhibit the same behavior. The amounts of S_f and S_{tot} are proportional to the second and third-order of Re, respectively.

References

[1] P. D. McCormack, H. Welker, and M. Kelleher, “Taylor-Goertler Vortices and Their Effect on Heat Transfer,” J. Heat Transfer, vol. 92, no. 1, p. 101, Feb. 1970.

[2] D. B. Tuckerman and R. F. W. Pease, “High-performance heat sinking for VLSI,” IEEE Electron Device Lett., vol. 2, no. 5, pp. 126–129, May 1981.

[3] Toh KC, Chen XY, Chai JC, Numerical computation of fluid flow and heat transfer in microchannels. Int J Heat Mass Transfer 45, 5133-5141, 2002

[4] Peng. XF, Peterson. GP, Convective heat transfer and flow friction for water flow in microchannels structures. Int J Heat Mass Tran 39: 2599-2608, 1996

[5] Peng XF, Peterson GP, The effect of thermofluid and geometrical parameters on convection of liquids through rectangular microchannels. Int J Heat Mass Tran 38: 755-758, 1995

[6] V.S. Duryodhan, A. Singh, S.G. Singh, A. Agrawal, Convective heat transfer in diverging and converging microchannels, Heat and Mass Transfer, Vol. 80, No.1, pp. 424-438, 2015.

[7] O. Pourmehran, M. Rahimi-Gorji, M. Hatami, S.A.R. Sahebi, G. Domairry, Numerical optimization of microchannel heat sink (MCHS) performance cooled by KKL based nanofluids in saturated porous

medium, the Taiwan Institute of Chemical Engineers, Vol. 55, pp. 49-68, 2015.

[8] M. Hatami, D. Ganji, Thermal and flow analysis of microchannel heat sink (MCHS) cooled by Cu-water nanofluid using porous media approach and least square method, Energy Conversion and management, Vol. 78, pp. 347-358, 2014

[9] P. A. K. Lam, K. A. Prakash, A numerical investigation of heat transfer and entropy generation during jet impingement cooling of protruding heat sources without and with porous medium, Energy Conversion and Management, Vol. 89, pp. 626-643, 2015.

[10] T. W. Ting, Y. M. Hung, N. Guo, Entropy generation of viscous dissipative nanofluid convection in asymmetrically heated porous microchannels with solid-phase heat generation, Energy Conversion and Management, Vol. 105, pp. 731-745, 2015.

[11] M. Kalteh, S.S. Abedinzadeh, Numerical investigation of MHD nanofluid forced convection in a microchannel using lattice Boltzmann method, Iranian Journal of Science and Technology, Transactions of Mechanical Engineering, 42(1), 23-34, 2018

[12] J. Guo, M. Xu, and L. Cheng, "Second law analysis of curved rectangular channels," Int. J. Therm. Sci., vol. 50, no. 5, pp. 760–768, May 2011.

[13] Hung, T. C., Yan, W. M., Wang, X. D., and Chang, C. Y., "Heat Transfer Enhancement in Microchannel Heat Sinks using Nanofluids", International Journal of Heat and Mass Transfer, Vol. 55, No.9, pp. 2559-2570, 2012.

[14] T.-C. Hung, W.-M. Yan, Effects of tapered-channel design on thermal performance of microchannel heat sink, International Communications in Heat and Mass Transfer, 39(9) 1342-1347, 2012

[15] Naphon, P., and Nakharintr, L., "Heat Transfer of Nanofluids in the Mini-rectangular Fin Heat Sinks", International Communications in Heat and Mass Transfer, Vol. 40, pp. 25-31, 2012.

[16] R. Chein, J. Chen, Numerical study of the inlet/ outlet arrangement effect on microchannel heat sink performance, International Journal of Thermal Sciences, 48(8), 1627-1638, 2009

[17] R. W. Knight, D. J. Hall, J. S. Goodling, and R. C. Jaeger, "Heat sink optimization with application to microchannels," IEEE Trans. Components, Hybrids, Manuf. Technol., vol. 15, no. 5, pp. 832–842, 1992.

[18] Selvakumar, P., and Suresh, S., "Convective Performance of CuO/Water Nanofluid in an Electronic Heat Sink", Experimental Thermal and Fluid Science, Vol. 40, pp. 57-63, 2012.

[19] Mostafa S, Ali K, Convective heat transfer and entropy generation analysis on Newtonian and non-Newtonian fluid flows between parallel-plates under slip boundary conditions. Int J Heat Mass Transfer, 70: p. 664-673, 2014

[20] H. Khorasanizadeh, M. Sepehrnia, Effects of different inlet/outlet arrangements on performance of a trapezoidal porous microchannel heat sink, Modares Mechanical Engineering, Vol. 16, No. 8, pp. 269-280, 2016. (in Persian)

[21] H. Khorasanizadch, M. Sepehrnia, R. Sadeghi, Three dimensional investigations of inlet/outlet arrangements and nanofluid utilization effects on a triangular microchannel heat sink performance, Modares Mechanical Engineering, Vol. 16, No. 12, pp. 27-38, 2016. (in Persian)

[22] S. E. Ghasemi, A. Ranjbar, M. Hosseini, Thermal and hydrodynamic characteristics of water-based suspensions of Al,O, nanoparticles in a novel minichannel heat sink, Journal of Molecular Liquids, Vol. 230, pp. 550-556, 2017

[23] L. Lin, J. Zhao, G. Lu, X.-D. Wang, and W.-M. Yan, "Heat transfer enhancement in microchannel heat sink by wavy channel with changing wavelength/amplitude," Int. J. Therm. Sci., vol. 118, pp. 423–434, Aug. 2017.

[24] A Nemati, H. Nami, M. Yari, S. F. Ranjbar, Energy and exergy analysis of a two-stage thermoelectric used for heating and cooling AmirKabir Mechanical Engineering, Articles in press, 2017. (in persian).

[25] L. Zhu, J. Yu, Optimization of heat sink of thermoelectric cooler using entropy generation analysis, International Journal of

Thermal Sciences, Vol. 118, No. 1, pp. 168-175. 2017.

[26] Delsman, E., et al., Microchannel plate geometry optimization for even flow distribution at high flow rates. Chemical Engineering Research and Design, 2004. 82(2): p. 267-273.

[27] Haddad, O., M. Abuzaid, and M. Al Nimr, Entropy generation due to laminar incompressible forced convection flow through parallel plates microchannel. Entropy, 2004. 6(5): p. 413-426.

[28] Chuan, L., et al., Fluid flow and heat transfer in microchannel heat sink based on porous fin design concept. International Communications in Heat and Mass Transfer, 2016 :p.65.5. 52-57.

[29] M. Shaeri, M. Yaghoubi, Numerical analysis of turbulent convection heat transfer from an array of perforated fins, International Journal of Heat and Fluid Flow, Vol. 30, No. 2, pp. 218-228, 2009

[30] L. Micheli, K. S. Reddy, T. K. Mallick, Experimental comparison of micro-scaled plate-fins and pin-fins under natural convection, International Communications in Heat and Mass Transfer, Vol. 75, pp. 59-66, 2016.

[31]A. Ebrahimi, F. Rikhtegar, A. Sabaghan, E. Roohi, Heat transfer and entropy generation in a microchannel with longitudinal vortex generators using nanofluids, Energy, Vol. 101, pp. 190-201, 2016.

[32] M. Hemmat Esfe, M. Afrand, S. Gharehkhani, H. Rostamian, D. Toghraie, and M. Dahari, "An experimental study on viscosity of alumina-engine oil: Effects of temperature and nanoparticles concentration," Int. Commun. Heat Mass Transf., vol. 76, pp. 202–208, Aug. 2016.

[33] A. A. A. A. Al-Rashed, A. Shahsavar, O. Rasooli, M. A. Moghimi, A. Karimipour, and M. D. Tran, "Numerical assessment into the hydrothermal and entropy generation characteristics of biological water-silver nano-fluid in a wavy walled microchannel heat sink," Int. Commun. Heat Mass Transf., vol. 104, pp. 118–126, May 2019.

[34] M. M. Sarafraz and F. Hormozi, "Intensification of forced convection heat transfer using biological nanofluid in a double-pipe heat exchanger," Exp. Therm. Fluid Sci., vol. 66, pp. 279–289, Sep. 2015.

[35] A. Sciacovelli, V. Verda, E. Sciubba, Entropy generation analysis as a design tool—A review, Renewable and Sustainable Energy Reviews 43, p: 1167–1181, 2015

[36] Advanced Engineering Thermodynamics Fourth Edition, Adrian Bejan, J. A. Jones Distinguished Professor Duke University Durham, North Carolina

[37] Y. Sui, P. S. Lee, and C. J. Teo, "An experimental study of flow friction and heat transfer in wavy microchannels with rectangular cross section, Int. J. Therm. Sci., vol. 50, no. 12, pp. 2473–2482, Dec. 2011.